PRAMANA
— journal of
physics

Vol. 66, No. 2
February 2006
pp. 389–401

Microscopic study of low-lying collective bands in ^{77}Kr

K C TRIPATHY[1], R SAHU[2] and S MISHRA[2]
[1]Department of Physics, North Orissa University, Baripada 757 003, India
[2]Physics Department, Berhampur University, Berhampur 760 007, India
E-mail: rankasahu@rediffmail.com

MS received 26 May 2005; revised 21 October 2005; accepted 18 November 2005

Abstract. The structure of the collective bands in ^{77}Kr is investigated within our deformed shell model (DSM) based on Hartree–Fock states. The different levels are classified into collective bands on the basis of their $B(E2)$ values. The calculated $K = 5/2^+$ ground band agrees reasonably well with the experiment. An attempt has been made to study the structure of the 3-quasiparticle band based on large J state in this nucleus. The calculated collective bands, the $B(E2)$, and $B(M1)$ values are compared with available experimental data. The nature of alignments in the low-lying bands is also analyzed.

Keywords. Deformed shell model; three-quasiparticle band; ^{77}Kr; energy spectrum; $B(E2)$ and $B(M1)$ values.

PACS Nos 21.10.-k; 21.60.Jz; 27.50.+e

1. Introduction

In the last few years, the spectroscopy of nuclei in the mass region $A = 80$ has been extensively investigated both theoretically and experimentally. The studies of these nuclei have been quite interesting, fascinating and often challenging. The nuclei in this region show a variety of nuclear phenomena such as large ground state deformation, coexistence of shapes, band crossing, rapid variation of nuclear structure with change in nucleon number, identical bands etc. The neutron deficient krypton [1], strontium [2] and zirconium [3] isotopes are known to have large ground state deformation. Hence the nuclei in this region have become a rich testing ground for both nuclear models and new experimental techniques. In particular, in neutron-deficient krypton nuclei, the protons and neutrons lie close to the midshell and hence they exhibit enhanced collectivity.

Extensive experimental studies of ^{77}Kr have recently been performed by Sylvan *et al* [4] and Johnson *et al* [5] (see also refs [6,7]). These experimental studies have resulted in the identification of positive parity and negative parity collective bands up to very high spin. The ground state for ^{77}Kr is based on $K = 5/2^+$ with the

$K = 3/2^-$ band lying higher in energy. In addition, a high K 3-quasiparticle band has been observed for this nucleus.

Nuclei in this region have been analyzed recently using several models: (i) excited Vampir variational approach based on HFB with realistic interactions is used to study yrast levels [8]; (ii) projected shell model (PSM) [9] with pairing plus quadrupole–quadrupole interaction and also quadrupole pairing is used to study ground band and quadrupole moments; (iii) Monte Carlo shell model [10] with pairing plus quadrupole–quadrupole interaction is used to study ground state quadrupole moments and occupancies. Various phenomenological models like interacting boson model, particle-rotor model etc. are also used to describe nuclei in this region. In the past several years we have been studying nuclei in this region using our deformed shell model [11–16]. Our microscopic model has been quite successful in describing many properties of the nuclei in this region. We have successfully described the spectroscopic properties of the neighbouring isotopes ^{78}Kr [14] and ^{76}Kr [15]. We have also described the 3-quasiparticle bands observed in ^{77,79,81}Br [12]. In view of the above, it would be quite interesting to study the structure of the collective bands observed in ^{77}Kr within our microscopic model.

In §2, we give a brief outline of the model. The results are discussed in §3. We summarize our results in section 4.

2. Theory

In our calculation, our basis space consists of the spherical orbitals $1p_{3/2}$, $0f_{5/2}$, $1p_{1/2}$ and $0g_{9/2}$ with ^{56}Ni as the inert core. The spherical single-particle energies of these orbitals relative to ^{56}Ni core are taken as 0.0, 0.78, 1.08 and 3.0 MeV respectively. We find from our experience that the odd A nuclei require smaller $g_{9/2}$ single particle energies ($E(g_{9/2})$) compared to their even–even neighbours. We have taken the spherical single particle energy of $g_{9/2}$ to be 4.25 MeV for ^{74,76}Kr [15]. The occupancy of the $g_{9/2}$ orbital for both ^{74,76}Kr and ^{77}Kr remains the same (except for the odd neutron) even though the single particle energy for the two cases are different. Thus (and also from our calculation) we find that for ^{77}Kr, the $g_{9/2}$ occupancy remains the same irrespective of whether we take $E(g_{9/2})$ to be 4.25 MeV or 3 MeV. We find that as long as the $g_{9/2}$ occupancy remains the same, varying E($g_{9/2}$) does not significantly change the relative spacing of the levels of given parity. It only affects the relative spacing of the negative parity bands with respect to the positive parity bands. Taking $E(g_{9/2}) = 3.0$ MeV reproduces correctly the interband spacing. Hence we take the spherical single particle energy of the $g_{9/2}$ to be 3.0 MeV. The effective interaction matrix elements, used here, have been given by Kuo and subsequently modified by Ahalpara *et al* [11]. This interaction has been quite successfully used by us in describing many important features of the nuclei in this region.

The details of the model have been described in our previous publications (see for example ref. [15]). For completeness, we give a few important steps. In the first place, the HF single particle equation is solved self-consistently and the lowest energy prolate intrinsic state is obtained. Then various excited intrinsic states are obtained by making particle–hole excitations over the lowest intrinsic state. A

constrained HF calculation (tagged HF) is performed in each case. These intrinsic states do not have good angular momenta. Hence good angular momentum states are projected from each of these intrinsic states. In general the good angular momentum states coming from different intrinsic states are not orthogonal to each other. Hence they are orthonormalized by performing a band mixing calculation.

Let the various intrinsic states obtained by solving the axially symmetric HF equation self-consistently be denoted by $\chi_K(\mu)$ with the μ distinguishing different intrinsic states with same K. Good angular momentum states are projected from each of these intrinsic states using the projection operator

$$P^J_{MK} = \frac{2J+1}{8\pi^2} \int D^{J^*}_{MK}(\Omega) R(\Omega) \mathrm{d}\Omega. \tag{1}$$

The angular momentum projected states ϕ^J_{MK} obtained from different intrinsic states have to be orthogonalized since they may not be orthogonal to each other. For this purpose, we consider the overlap matrix

$$N^J_{K'\mu',K\mu} = \langle \phi^J_{MK'}(\mu') | \phi^J_{MK}(\mu) \rangle. \tag{2}$$

For an orthonormal set of vectors, this matrix would be a unit matrix, whereas in the case of the non-orthogonal basis, it is not diagonal. Hence the matrix $N^J_{K'\mu',K\mu}$ is diagonalized and the resulting vectors can be written as

$$\Phi^J_M(\alpha) = \sum_{K\mu} S^J_{K\alpha}(\mu) \phi^J_{MK}(\mu), \tag{3}$$

where

$$S^J_{K\alpha}(\mu) = \left[n^J_M(\alpha) \right]^{-1/2} X^J_{K\alpha}(\mu) \tag{4}$$

with $X^J_{K\alpha}$ corresponding to the element of the unitary transformation matrix that diagonalizes the overlap matrix N^J and n^J_M denotes the eigenvalues of N^J. The function $\Phi^J_M(\alpha)$ constitutes an orthonormal set of vectors. The composite spectrum of a nucleus is obtained by diagonalizing the Hamiltonian matrix in the basis of these orthonormalized projected states. The overlap

$$B^J_K(\eta,\alpha) = \langle \phi^J_{MK}(\eta) | \Phi^J_M(\alpha) \rangle = \sum_{K_1\eta_1} S^J_{K_1\eta_1}(\alpha) N^J_{K\eta,K_1\eta_1} \tag{5}$$

gives the measure of the state $\phi^J_{MK}(\eta)$ projected from a given intrinsic state $\chi_K(\eta)$ that the eigenstate $\Phi^J_M(\alpha)$ contains. The larger the amplitude $|B^J_K(\eta,\alpha)|^2$, the more pronounced will be the characteristic of that parent intrinsic state in the state $\Phi^J_M(\alpha)$.

The calculations of electric and magnetic transition probabilities between the states $\Phi^J_M(\alpha)$ involve the evaluation of the matrix elements of the appropriate transition operators O^l_m of rank l between these states.

In figure 1, the single particle levels corresponding to the lowest prolate intrinsic HF states are given. The protons are represented by the circles and the neutrons by crosses. For odd A nuclei, the time reversal symmetry in the HF solutions is

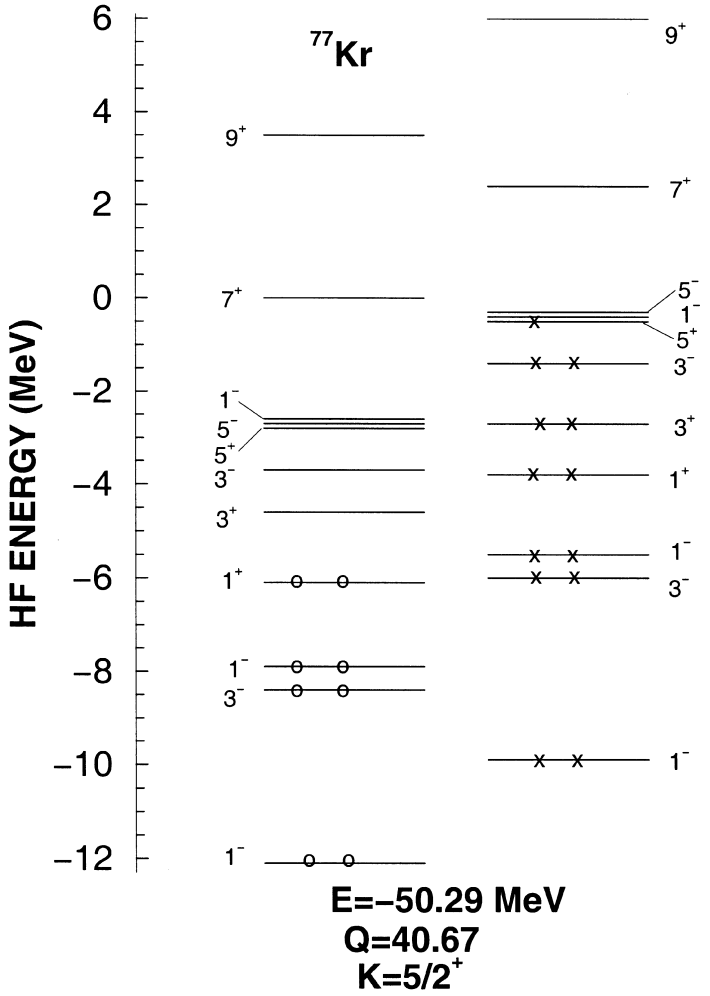

Figure 1. The single particle spectrum for the lowest $K = 0^+$ prolate HF intrinsic state. The protons are represented by circles and the neutrons by crosses. The numbers next to the levels denote 2 k values. The positive parity levels are represented by a plus sign. All other levels have negative parity. The HF energy in MeV and mass quadrupole moment in the unit of b^2 are also shown. The square of oscillator length parameter b^2 is taken to be $1.01 \times A^{1/3}$ fm^2.

broken, so that single particle energies of the states $|k\rangle$ and the time reversed states $|-k\rangle$ are not degenerate. However, in actual practice, the difference between the two energies is quite small and we have ignored them in drawing the figure and showing the occupancies of the deformed states. However in actual calculations, the exact energies are taken into account.

An analysis of the HF single-particle spectrum shows that six protons are distributed in the p-f single-particle orbits and two protons are in the $g_{9/2}$ orbits. There is a well-defined gap of about 1.5 MeV above the proton Fermi surface. Five neutrons occupy the $g_{9/2}$ single-particle orbits and the rest are distributed in p-f orbits. The last neutron occupies the $k = 5/2^+$ orbit so that the lowest HF solution has $K = 5/2^+$. However, very close to $k = 5/2^+$, there are two negative parity-single particle orbits namely $k = 1/2^-$ and $k = 5/2^-$. Therefore negative parity solutions are expected to be very close in energy. Actual calculation shows that the HF solution with $K = 1/2^-$ and $K = 5/2^-$ are only 0.1 and 0.8 MeV above the lowest solution. The observed low-lying negative parity collective bands are expected to arise from the neutron excitations only since there is relatively large gap above the proton Fermi surface and hence proton excitations will lie high in energy.

For calculating positive parity states, we have taken ten low-lying prolate intrinsic states. Of these, one has $K = 1/2^+$, two have $K = 3/2^+$, four intrinsic states have $K = 5/2^+$, one with $K = 7/2^+$ and two with $K = 9/2^+$. The proton aligned band with $K = 7/2^+$ and $K = 5/2^+$ are obtained by placing the last two protons in $k = 3/2^+$ and $k = 1/2^+$ orbits. Two neutron aligned bands with $K = 9/2^+$ are obtained by placing the two valance neutrons in $k = 3/2^+$ and $k = 1/2^+$. Good angular momentum states are projected from each of these intrinsic states and then a band mixing calculation is performed to obtain the bands of positive-parity states.

The intrinsic states with negative parity are obtained by making 1p-1h excitations to the $0g_{9/2}$ orbital from the lowest prolate solution and then performing a constrained HF calculation. We have considered 12 such excited intrinsic states. Of these, one has $K = 1/2^-$, three have $K = 3/2^-$, one with $K = 5/2^-$ and one intrinsic state has $K = 7/2^-$. In addition, we have considered three 3-quasiparticle configurations with $K = 13/2^-$ and three 5-quasiparticle configurations with $K = 15/2^-$. As described above, good angular momentum states are projected from each of these intrinsic states and then a band-mixing calculation is performed.

It should be emphasized that the deformed HF calculations in a limited configuration space are essentially to approximate a full shell-model calculation [17]. In our work, the HF calculation in a limited configuration space is used to generate a deformed shell-model basis, wherein a few low-lying configurations are then sufficient to give most of the essential features and systematics of spectroscopic properties. This is not HF in its general sense, as used by people who work with Skyrme and other general interaction where shell gap plays a crucial role.

In our calculation, we do not consider oblate HF intrinsic states as they are not likely to occur in the ground state domain in this region. The reason for ignoring the oblate intrinsic states in strontium isotopes have been discussed in detail in our earlier publication [13]. We find in our band mixing calculation that oblate states do not mix in any significant way with the prolate states and thus do not affect the results for spectroscopic or electromagnetic transitions. We, therefore, consider only prolate or spherical intrinsic states.

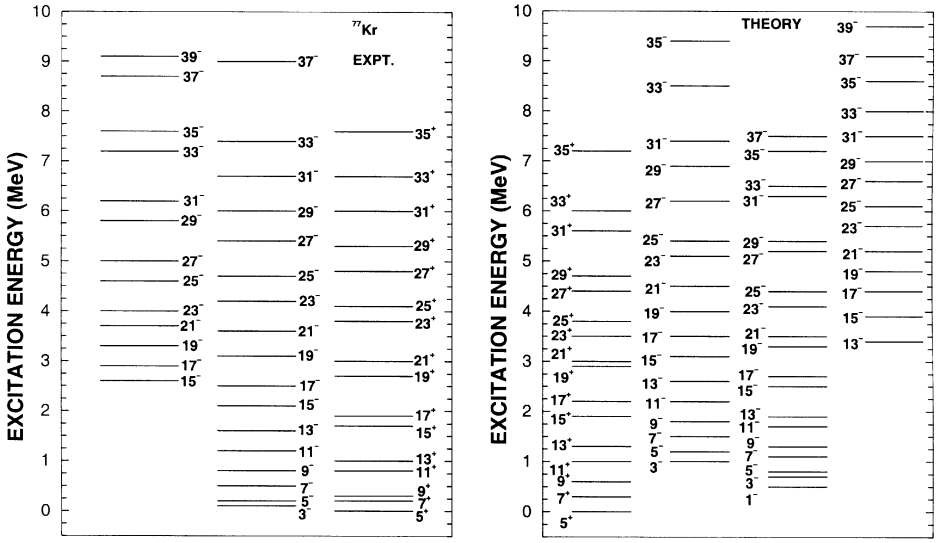

Figure 2. The different collective bands obtained from our DSM calculation are compared with the experimental collective bands. The numbers next to the energy levels give 2 J values. The data are taken from ref. [5].

3. Results

The calculated levels are classified into different collective bands on the basis of the $E2$ transition probabilities between them. The principle is that interband transition probabilities are smaller than intraband transition probabilities by an order of magnitude. Hence all the levels connected by strong $B(E2)$s are classified into one band. All these levels also have similar structures.

3.1 *Energy spectra*

The calculated levels are compared with experiment in figure 2. As has been shown in figure 1, the HF energy for the lowest configuration is 50.29 MeV. After performing angular momentum projection and band mixing, the lowest energy state which is $J = 5/2^+$ is at 52.35 MeV. Thus there is an extra correction of around 2 MeV due to angular momentum projection and band mixing. The experimental data are taken from refs [4–7]. Our calculation gives $K = 5/2^+$ as the ground band in agreement with experiment. The staggering of the levels are correctly reproduced in this band. This band mainly originates from the lowest $K = 5/2^+$ intrinsic state. However, as we go to higher spin states, the mixing increases. We find that a proton-aligned band originating mainly from the intrinsic state with $K = 7/2^+$ crosses the ground band and becomes yrast at $J = 23/2^+$. At $J = 29/2^+$, there is no clear cut band crossing, but in the wave function, the probability of the neutron-aligned intrinsic state is relatively large. To test whether our predictions

are correct, we have calculated the magnetic moments. If the magnetic moment of a level increases suddenly, then we can conclude that there is proton alignment. If, however, there is a decrease in magnetic moment, then the alignment is due to neutrons. The calculated values of the magnetic moment are given in table 1. We find that the magnetic moment suddenly increases at $J = 23/2^+$ confirming that there is a proton alignment. Again at $J = 29/2^+$, the magnetic moment suddenly decreases indicating that there is an alignment of neutron. From the analysis of the experimental data, Sylvan *et al* [4] have come to the conclusion that there occurs two band crossings, one due to proton alignment and the other due to neutron alignment. This is in agreement with our predictions. Measurement of the g-factor will confirm our conjecture about the nature of the band crossing. The calculated $K = 3/2^-$ excited band lies about 1 MeV higher compared to experiment. However the relative spacing of the levels is nicely reproduced. The staggering of the levels is reproduced for this band also. However, we do not see any band crossing for this band. The analysis of the calculated magnetic moment given in table 1 shows a slow monotonic increase in magnetic moment confirming our above predictions. Sylvan *et al* [4] have predicted a band crossing for this band. The measurement of g-factor will be quite useful in determining the alignment.

In addition we have predicted a low-lying negative parity band with $K = 1/2^-$. This band has not been identified experimentally. Unlike the $K = 3/2^-$ band which decays to the $J = \frac{5}{2}^+$ level of the ground band by $E1$, the $K = 1/2^-$ band can only decay to the band head of the positive parity ground band with a multipolarity $E3$ or $M2$ which are weak. Experimentally [18] a $\frac{1}{2}^-$ level has been identified at 459.9 keV for this nucleus which can be taken as the band head of our predicted $K = 1/2^-$ band. However, in our calculation this band comes very low, below the $K = 3/2^-$ band. Larger basis space with the inclusion of the higher $1d_{5/2}$ and $0g_{7/2}$ orbits will probably produce sufficient collectivity and push up the $K = 1/2^-$ band.

3.2 *Three-quasiparticle bands*

Sylvan *et al* [4] have observed a negative parity band starting at around 2.6 MeV with $J = 15/2^-$. This band is somewhat different from the 3-quasiparticle bands observed in this region. Unlike other 3-quasiparticle bands, this band exhibits collectivity and $E2$ decays are large. To describe this band within our microscopic model, we constructed 3-quasiparticle bands with high spin in the following three ways [12]:

(a) By placing the odd neutron in $k = 5/2^+$ and the two valence protons in $k = 5/2^+$ and $k = 3/2^-$.
(b) By placing the odd neutron in $k = 5/2^-$ and the two valence protons in $k = 5/2^+$ and $k = 3/2^+$.
(c) By placing the three valence neutrons in the orbits $k = 5/2^-$, $k = 5/2^+$ and $k = 3/2^+$.

All the HF configurations constructed in the above method gives the azimuthal quantum number $K = 13/2^-$. Since in the experiment, this band starts at $15/2^-$,

Table 1. Deformed HF predictions for quadrupole moment (efm^2) and magnetic moment (n.m.) for different states.

KJ	QM	MM
$5/2^+$ $5/2^+$	92.4	−0.97
$5/2^+$ $7/2^+$	13.6	−0.27
$5/2^+$ $9/2^+$	−28.1	0.12
$5/2^+$ $11/2^+$	−54.8	1.21
$5/2^+$ $13/2^+$	−70.3	1.55
$5/2^+$ $15/2^+$	−81.6	4.86
$5/2^+$ $17/2^+$	−89.4	6.64
$5/2^+$ $19/2^+$	−102.5	18.97
$5/2^+$ $21/2^+$	−107.7	19.33
$5/2^+$ $23/2^+$	−135.3	29.97
$5/2^+$ $25/2^+$	−119.2	24.37
$5/2^+$ $27/2^+$	−160.0	35.78
$5/2^+$ $29/2^+$	−68.4	−7.76
$5/2^+$ $31/2^+$	−188.6	43.93
$5/2^+$ $33/2^+$	−167.0	40.50
$3/2^-$ $3/2^-$	50.6	0.43
$3/2^-$ $5/2^-$	76.3	1.6
$3/2^-$ $7/2^-$	−11.3	3.1
$3/2^-$ $9/2^-$	−25.9	4.07
$3/2^-$ $11/2^-$	−60.5	3.66
$3/2^-$ $13/2^-$	−59.3	6.5
$3/2^-$ $15/2^-$	−78.8	7.96
$3/2^-$ $17/2^-$	−72.7	8.97
$3/2^-$ $19/2^-$	−88.9	10.35
$3/2^-$ $21/2^-$	−78.9	11.5
$3/2^-$ $23/2^-$	−97.9	12.55
$3/2^-$ $25/2^-$	−82.4	14.29
$3/2^-$ $27/2^-$	−103.2	14.22
$3/2^-$ $29/2^-$	−85.2	17.66
$3/2^-$ $31/2^-$	−44.7	19.71
$3/2^-$ $33/2^-$	−89.5	21.69

we tried to construct HF configurations with $K = 15/2^-$. However, within the model space, we cannot have HF configurations with $K = 15/2^-$ if we restrict ourselves to only 3-quasiparticle excitations. However, excited configurations with $K = 15/2^-$ can be constructed with 5-quasiparticle excitations. We consider three such excitations as given below:

(a) By placing the three valence neutrons in $k = 5/2^-$, $k = 5/2^+$ and $k = 3/2^-$ and two valence protons in $k = 5/2^+$ and $k = -3/2^-$.
(b) By placing the three valence neutrons in $k = 1/2^-$, $k = 3/2^+$ and $k = 3/2^-$ and two valence protons in $k = 5/2^+$ and $k = 3/2^-$.
(c) By placing the three valence neutrons in $k = 5/2^-$, $k = 1/2^-$ and $k = 5/2^+$ and two valence protons in $k = 3/2^-$ and $k = 1/2^+$.

We performed angular momentum projection and band mixing calculation considering these configurations along with the other low-lying intrinsic configurations as discussed before. The results for the lowest high-spin negative parity states are presented in figure 2. We find that the band obtained after angular momentum projection and band mixing and originating mainly from the intrinsic state (c) given above with $K = 13/2^-$ is lowest in energy and is plotted in figure 2. From $J = 15/2^-$, the agreement with experiment for this band is quite satisfactory. Similar results were obtained for ^{77}Br in our earlier calculation [12]. In ^{77}Br also, the high J negative parity state starts at $15/2^-$ and we described it in terms of a 3-quasiparticle band with $K = 13/2^-$. The $K = 15/2^-$ bands which are 5-quasiparticle in nature lie much higher in energy. There is a lot of difference in the structure of this band compared to bromine isotopes. Whereas in bromine isotopes, the 3-quasiparticle bands were built by exciting one proton and two neutrons, in ^{77}Kr the 3-quasiparticle band is built completely by particle–hole excitation of neutrons only as described in the construction (c) above. The description about the $B(E2)$ and $B(M1)$ values for the transitions within this band are given in the next subsection. The intrinsic state from which this band mainly originates has quadrupole deformation of $\beta = 0.25$. The value of β is extracted from the calculated intrinsic quadrupole moment using the well-known formula $Q_{\rm HF} = \frac{3}{\sqrt{5\pi}} ZR_0^2\beta$ with $R_0 = 1.3A^{1/3}$ fm.

3.3 *Electromagnetic properties*

In the calculation of $B(E2)$ values, we have taken the effective charge of the proton to be $1.6e$ and that of the neutron to be $1.0e$. These effective charges were used in our earlier calculations also. We have calculated $B(E2)$ values for all possible transitions for this nucleus. Some of the $B(E2)$ values are given in table 2. Except for a few transitions, the present calculation reproduces the experimental values quite satisfactorily. The calculated $B(M1)$ values are also tabulated in table 2. In the calculation of the $B(M1)$ values, we have used bare gyromagnetic ratios. Most of the experimental $B(M1)$ values are reproduced in our calculation within a factor of 3. For the 3-quasiparticle band, we find that the $B(M1)$ values are larger by a factor of around 5 compared to the $B(M1)$ values for the low-lying bands. The $B(E2)$ values for this band is comparable to those for the low-lying bands unlike the 3-quasiparticle bands observed in other nuclei in this region.

The calculated quadrupole moment and magnetic moment for the low-lying bands are given in table 1. There are no experimental values to compare.

4. Summary

The spectroscopic properties of ^{77}Kr are calculated within the deformed shell model. In our calculation, the $K = 5/2^+$ band is the ground band in agreement with experiment. The staggering of the levels are well-reproduced. We predict two band crossings for this band, the first one due to alignment of proton and the other due to alignment of neutron. The calculated magnetic moment supports the

Table 2. Deformed HF model predictions for $B(E2;K_iJ_i \rightarrow K_fJ_f)$ in W.u. and $B(M1;K_iJ_i \rightarrow K_fJ_f)$ in μ_N^2 for ^{77}Kr are compared with experimental data. The experimental data are from ref. [5].

$B(E2)$				$B(M1)$			
K_iJ_i	K_fJ_f	DSM	Expt.	K_iJ_i	K_fJ_ff	DSM	Expt.
$5/2^+$ $7/2^+$	$5/2^+$ $5/2^+$	102.0		$5/2^+$ $7/2^+$	$5/2^+$ $5/2^+$	0.28	
$5/2^+$ $9/2^+$	$5/2^+$ $5/2^+$	30.2	21^{+5}_{-3}	$5/2^+$ $9/2^+$	$5/2^+$ $7/2^+$	0.45	$0.12^{+0.01}_{-0.01}$
$5/2^+$ $9/2^+$	$5/2^+$ $7/2^+$	83.8		$5/2^+$ $11/2^+$	$5/2^+$ $9/2^+$	0.45	$0.16^{+0.03}_{-0.04}$
$5/2^+$ $11/2^+$	$5/2^+$ $7/2^+$	50.4	72^{+18}_{-12}	$5/2^+$ $13/2^+$	$5/2^+$ $11/2^+$	0.70	$0.30^{+0.07}_{-0.13}$
$5/2^+$ $11/2^+$	$5/2^+$ $9/2^+$	60.6	56^{+23}_{-19}	$5/2^+$ $15/2^+$	$5/2^+$ $13/2^+$	0.57	$0.12^{+0.02}_{-0.03}$
$5/2^+$ $13/2^+$	$5/2^+$ $9/2^+$	64.4	70^{+47}_{-20}	$5/2^+$ $17/2^+$	$5/2^+$ $15/2^+$	1.17	$0.41^{+0.07}_{-0.10}$
$5/2^+$ $13/2^+$	$5/2^+$ $11/2^+$	45.9	4^{+12}_{-4}	$5/2^+$ $19/2^+$	$5/2^+$ $17/2^+$	1.15	$0.14^{+0.03}_{-0.06}$
$5/2^+$ $15/2^+$	$5/2^+$ $11/2^+$	69.6	58^{+5}_{-10}	$5/2^+$ $21/2^+$	$5/2^+$ $19/2^+$	1.75	$0.55^{+0.10}_{-0.15}$
$5/2^+$ $15/2^+$	$5/2^+$ $13/2^+$	32.0	9^{+5}_{-4}	$5/2^+$ $23/2^+$	$5/2^+$ $21/2^+$	1.72	$0.18^{+0.03}_{-0.06}$
$5/2^+$ $17/2^+$	$5/2^+$ $13/2^+$	76.2	110^{+27}_{-18}	$5/2^+$ $25/2^+$	$5/2^+$ $23/2^+$	1.66	$0.51^{+0.08}_{-0.12}$
$5/2^+$ $17/2^+$	$5/2^+$ $15/2^+$	27.6	37^{+78}_{-34}	$5/2^+$ $27/2^+$	$5/2^+$ $25/2^+$	1.21	$0.24^{+0.04}_{-0.06}$
$5/2^+$ $19/2^+$	$5/2^+$ $15/2^+$	60.3	32^{+8}_{-6}	$5/2^+$ $29/2^+$	$5/2^+$ $27/2^+$	1.78	$0.46^{+0.08}_{-0.13}$
$5/2^+$ $19/2^+$	$5/2^+$ $17/2^+$	18.0	17^{+10}_{-7}	$5/2^+$ $31/2^+$	$5/2^+$ $29/2^+$	0.46	> 0.24
$5/2^+$ $21/2^+$	$5/2^+$ $17/2^+$	70.6	122^{+34}_{-22}	$5/2^+$ $33/2^+$	$5/2^+$ $31/2^+$	2.42	$1.02^{+0.20}_{-0.34}$
$5/2^+$ $21/2^+$	$5/2^+$ $19/2^+$	22.2		$1/2^-$ $3/2^-$	$1/2^-$ $1/2^-$	0.22	
$5/2^+$ $23/2^+$	$5/2^+$ $19/2^+$	72.0	53^{+13}_{-9}	$1/2^-$ $5/2^-$	$1/2^-$ $3/2^-$	0.03	
$5/2^+$ $23/2^+$	$5/2^+$ $21/2^+$	16.1	14^{+8}_{-6}	$1/2^-$ $7/2^-$	$1/2^-$ $5/2^-$	0.10	
$5/2^+$ $25/2^+$	$5/2^+$ $21/2^+$	80.5	112^{+26}_{-18}	$1/2^-$ $9/2^-$	$1/2^-$ $7/2^-$	0.02	
$5/2^+$ $25/2^+$	$5/2^+$ $23/2^+$	16.6	13^{+6}_{-13}	$1/2^-$ $11/2^-$	$1/2^-$ $9/2^-$	0.09	
$5/2^+$ $27/2^+$	$5/2^+$ $23/2^+$	79.2	98^{+26}_{-17}	$1/2^-$ $13/2^-$	$1/2^-$ $11/2^-$	0.01	
$5/2^+$ $27/2^+$	$5/2^+$ $25/2^+$	11.6	3^{+5}_{-3}	$1/2^-$ $15/2^-$	$1/2^-$ $13/2^-$	0.1	
$5/2^+$ $29/2^+$	$5/2^+$ $25/2^+$	82.7	44^{+12}_{-8}	$1/2^-$ $17/2^-$	$1/2^-$ $15/2^-$	0.01	
$5/2^+$ $29/2^+$	$5/2^+$ $27/2^+$	11.7	0^{+5}_{-0}	$1/2^-$ $19/2^-$	$1/2^-$ $17/2^-$	0.1	
$5/2^+$ $31/2^+$	$5/2^+$ $27/2^+$	77.5	> 8	$1/2^-$ $21/2^-$	$1/2^-$ $19/2^-$	0.008	
$5/2^+$ $31/2^+$	$5/2^+$ $29/2^+$	6.6		$1/2^-$ $23/2^-$	$1/2^-$ $21/2^-$	0.09	
$5/2^+$ $33/2^+$	$5/2^+$ $29/2^+$	81.2	81^{+27}_{-16}	$1/2^-$ $25/2^-$	$1/2^-$ $23/2^-$	0.007	
$5/2^+$ $33/2^+$	$5/2^+$ $31/2^+$	9.1		$1/2^-$ $27/2^-$	$1/2^-$ $25/2^-$	0.02	
$5/2^+$ $35/2^+$	$5/2^+$ $31/2^+$	54.2		$3/2^-$ $5/2^-$	$3/2^-$ $3/2^-$	0.9	$0.17^{+0.01}_{-0.02}$
$1/2^-$ $3/2^-$	$1/2^-$ $1/2^-$	51.2		$3/2^-$ $7/2^-$	$3/2^-$ $5/2^-$	0.77	$0.31^{+0.05}_{-0.08}$
$1/2^-$ $5/2^-$	$1/2^-$ $1/2^-$	51.6		$3/2^-$ $9/2^-$	$3/2^-$ $7/2^-$	0.88	$0.26^{+0.04}_{-0.06}$
$1/2^-$ $5/2^-$	$1/2^-$ $3/2^-$	13.9		$3/2^-$ $11/2^-$	$3/2^-$ $9/2^-$	0.92	$0.31^{+0.05}_{-0.08}$
$1/2^-$ $7/2^-$	$1/2^-$ $3/2^-$	56.0		$3/2^-$ $13/2^-$	$3/2^-$ $11/2^-$	1.01	$0.28^{+0.05}_{-0.07}$
$1/2^-$ $7/2^-$	$1/2^-$ $5/2^-$	6.2		$3/2^-$ $15/2^-$	$3/2^-$ $13/2^-$	1.0	$0.16^{+0.03}_{-0.04}$
$1/2^-$ $9/2^-$	$1/2^-$ $5/2^-$	72.9		$3/2^-$ $17/2^-$	$3/2^-$ $15/2^-$	1.1	$0.20^{+0.03}_{-0.05}$
$1/2^-$ $9/2^-$	$1/2^-$ $7/2^-$	6.3		$3/2^-$ $19/2^-$	$3/2^-$ $17/2^-$	1.04	$0.10^{+0.02}_{-0.02}$
$1/2^-$ $11/2^-$	$1/2^-$ $7/2^-$	73.2		$3/2^-$ $21/2^-$	$3/2^-$ $19/2^-$	1.14	
$1/2^-$ $11/2^-$	$1/2^-$ $9/2^-$	3.4		$3/2^-$ $23/2^-$	$3/2^-$ $21/2^-$	0.96	$0.08^{+0.01}_{-0.02}$
$1/2^-$ $13/2^-$	$1/2^-$ $9/2^-$	80.0		$3/2^-$ $25/2^-$	$3/2^-$ $23/2^-$	1.0	
$1/2^-$ $13/2^-$	$1/2^-$ $11/2^-$	3.6		$3/2^-$ $27/2^-$	$3/2^-$ $25/2^-$	0.8	
$1/2^-$ $15/2^-$	$1/2^-$ $11/2^-$	80.9		$13/2^-$ $15/2^-$	$13/2^-$ $13/2^-$	1.5	

Table 2. (contd.)

$B(E2)$				$B(M1)$			
K_iJ_i	K_fJ_f	DSM	Expt.	K_iJ_i	K_fJ_ff	DSM	Expt.
$1/2^-$ $15/2^-$	$1/2^-$ $13/2^-$	1.9		$13/2^-$ $17/2^-$	$13/2^-$ $15/2^-$	2.6	
$1/2^-$ $17/2^-$	$1/2^-$ $13/2^-$	82.7		$13/2^-$ $19/2^-$	$13/2^-$ $17/2^-$	3.5	
$1/2^-$ $17/2^-$	$1/2^-$ $15/2^-$	2.2		$13/2^-$ $21/2^-$	$13/2^-$ $19/2^-$	4.2	
$1/2^-$ $19/2^-$	$1/2^-$ $15/2^-$	83.4		$13/2^-$ $23/2^-$	$13/2^-$ $21/2^-$	4.7	
$1/2^-$ $19/2^-$	$1/2^-$ $17/2^-$	1.1		$13/2^-$ $25/2^-$	$13/2^-$ $23/2^-$	5.0	
$1/2^-$ $21/2^-$	$1/2^-$ $17/2^-$	82.8		$13/2^-$ $27/2^-$	$13/2^-$ $25/2^-$	5.2	
$1/2^-$ $21/2^-$	$1/2^-$ $19/2^-$	1.5		$13/2^-$ $29/2^-$	$13/2^-$ $27/2^-$	5.3	
$1/2^-$ $23/2^-$	$1/2^-$ $19/2^-$	82.3		$13/2^-$ $31/2^-$	$13/2^-$ $29/2^-$	5.2	
$1/2^-$ $23/2^-$	$1/2^-$ $21/2^-$	0.6					
$3/2^-$ $5/2^-$	$3/2^-$ $3/2^-$	109.8					
$3/2^-$ $7/2^-$	$3/2^-$ $3/2^-$	69.6					
$3/2^-$ $7/2^-$	$3/2^-$ $5/2^-$	92.8					
$3/2^-$ $9/2^-$	$3/2^-$ $5/2^-$	112.6	112^{+28}_{-19}				
$3/2^-$ $9/2^-$	$3/2^-$ $7/2^-$	46.4	14^{+12}_{-8}				
$3/2^-$ $11/2^-$	$3/2^-$ $7/2^-$	80.2	103^{+26}_{-17}				
$3/2^-$ $11/2^-$	$3/2^-$ $9/2^-$	32.3	51^{+22}_{-18}				
$3/2^-$ $13/2^-$	$3/2^-$ $9/2^-$	87.8	121^{+29}_{-20}				
$3/2^-$ $13/2^-$	$3/2^-$ $11/2^-$	23.9	19^{+8}_{-6}				
$3/2^-$ $15/2^-$	$3/2^-$ $11/2^-$	92.4	66^{+17}_{-11}				
$3/2^-$ $15/2^-$	$3/2^-$ $13/2^-$	17.8					
$3/2^-$ $17/2^-$	$3/2^-$ $13/2^-$	95.5	88^{+22}_{-14}				
$3/2^-$ $17/2^-$	$3/2^-$ $15/2^-$	14.3					
$3/2^-$ $19/2^-$	$3/2^-$ $15/2^-$	96.5	52^{+13}_{-18}				
$3/2^-$ $19/2^-$	$3/2^-$ $17/2^-$	11.5					
$3/2^-$ $21/2^-$	$3/2^-$ $17/2^-$	96.4	> 60				
$3/2^-$ $21/2^-$	$3/2^-$ $19/2^-$	9.8					
$3/2^-$ $23/2^-$	$3/2^-$ $19/2^-$	91.7	152^{+34}_{-23}				
$3/2^-$ $23/2^-$	$3/2^-$ $21/2^-$	8.4					
$3/2^-$ $25/2^-$	$3/2^-$ $21/2^-$	91.4					
$3/2^-$ $25/2^-$	$3/2^-$ $23/2^-$	8.4					
$3/2^-$ $27/2^-$	$3/2^-$ $23/2^-$	89.4	> 53				
$13/2^-$ $15/2^-$	$13/2^-$ $13/2^-$	74.0					
$13/2^-$ $17/2^-$	$13/2^-$ $13/2^-$	37.6					
$13/2^-$ $17/2^-$	$13/2^-$ $15/2^-$	82.0					
$13/2^-$ $19/2^-$	$13/2^-$ $15/2^-$	18.8					
$13/2^-$ $19/2^-$	$13/2^-$ $17/2^-$	81.8					
$13/2^-$ $21/2^-$	$13/2^-$ $17/2^-$	27.8					
$13/2^-$ $21/2^-$	$13/2^-$ $19/2^-$	75.4					
$13/2^-$ $23/2^-$	$13/2^-$ $19/2^-$	35.2					
$13/2^-$ $23/2^-$	$13/2^-$ $21/2^-$	67.5					
$13/2^-$ $25/2^-$	$13/2^-$ $21/2^-$	41.0					
$13/2^-$ $25/2^-$	$13/2^-$ $23/2^-$	59.8					
$13/2^-$ $27/2^-$	$13/2^-$ $23/2^-$	44.7					
$13/2^-$ $27/2^-$	$13/2^-$ $25/2^-$	52.4					

Table 2. (contd.)

$B(E2)$				$B(M1)$			
K_iJ_i	K_fJ_f	DSM	Expt.	K_iJ_i	K_fJ_ff	DSM	Expt.
$13/2^-$ $29/2^-$	$13/2^-$ $25/2^-$	46.5					
$13/2^-$ $29/2^-$	$13/2^-$ $27/2^-$	44.5					
$13/2^-$ $31/2^-$	$13/2^-$ $27/2^-$	47.0					
$13/2^-$ $31/2^-$	$13/2^-$ $29/2^-$	40.2					
$13/2^-$ $33/2^-$	$13/2^-$ $29/2^-$	83.8					

predicted nature of alignment. Sylvan *et al* [4] have come to the conclusion from their experimental analysis that there exist two band crossings as we have predicted. The calculated $K = 3/2^-$ band lies about 1 MeV higher but the relative spacing of the levels are well-reproduced. We do not find any band crossing in this band. The calculated magnetic moment do not show any sudden increase or decrease in the magnetic moment implying that there is no band crossing. The calculated 3-quasiparticle band compare well with experiment. We find that the observed levels are a part of the $K = 13/2^-$ band. The calculated $B(M1)$ values among the levels of this band are about 5 times larger than those between the low-lying levels. This band shows reasonably large collectivity with $\beta = 0.25$. The calculated $B(E2)$ values for the low-lying levels agree reasonably with experiment.

In future, we should expand the basis space so that we can calculate the energy levels up to higher angular momentum. For this, we should develop a proper effective interaction for the expanded basis space. This is a project for the future.

Acknowledgements

One of us (RS) is thankful to the Department of Science and Technology, Government of India for financial support.

References

[1] S L Tabor, P D Cottle, J W Holcomb, T D Johnson, P C Womble, S G Buccino and F E Durham, *Phys. Rev.* **C41**, 2658 (1990)
[2] C J Lister, P J Ennis, A A Chisti, B J Varley, W Gelletly, H G Price and A N James, *Phys. Rev.* **C42**, R1191 (1990)
[3] C J Lister *et al*, *Phys. Rev. Lett.* **59**, 1270 (1987)
[4] G N Sylvan *et al*, *Phys. Rev.* **C56**, 772 (1996)
[5] T D Johnson, J W Holcomb, P C Womble, P D Cottle, S L Tabor, F E Durham, S G Buccino and M Matsuzaki, *Phys. Rev.* **C42**, 2418 (1990)
[6] C J Gross, P D Cottle, D M Headly, U J Hüttmeier, E F Moore, S L Tabor and W Nazarewicz, *Phys. Rev.* **C36**, 2601 (1987)
[7] B Wörmann, K P Lieb, R Diller, L Lühmann, J Keinonen, L Cleemann and J Eberth, *Nucl. Phys.* **A431**, 170 (1984)

[8] A Petrovici, K W Schmid and A Faessler, *Nucl. Phys.* **A708**, 190 (2002); **A710**, 246 (2002)
[9] R Palit, J A Sheikh, Y Sun and H C Jain, *Nucl. Phys.* **A686**, 141 (2001)
[10] K Langanke, D J Dean and W Nazarewicz, *Nucl. Phys.* **A728**, 109 (2003)
[11] D P Ahalpara, K H Bhatt and R Sahu, *J. Phys.* **G11**, 735 (1985)
[12] R Sahu and S P Pandya, *Nucl. Phys.* **A529**, 20 (1991)
[13] K C Tripathy and R Sahu, *J. Phys.* **G20**, 911 (1994)
[14] K C Tripathy and R Sahu, *Nucl. Phys.* **A597**, 177 (1996)
[15] K C Tripathy and R Sahu, *J. Phys.* **G26**, 1271 (2000)
[16] R Sahu and V K B Kota, *Phys. Rev.* **C67**, 054323 (2003)
[17] S B Khadkikar, S C K Nair and S P Pandya, *Phys. Lett.* **B36**, 290 (1971)
S B Khadkikar, D R Kulkarni and S P Pandya, *Pramana – J. Phys.* **2**, 259 (1974)
[18] A R Farhan and B Singh, *Nucl. Data Sheet* **81**, 417 (1997)